Trop J Nat Prod Res, August 2025; 9(8): 3794 - 3801 **ISSN 2616-0684 (Print)**
ISSN 2616-0692 (Electronic)

Tropical Journal of Natural Product Research

Available online at https://www.tjnpr.org

Original Research Article

Thiolated Chitosan Nanoparticles as a Promising Mucoadhesive Polymer in a Nose-to-Brain Delivery System: A Biodistribution Study in Mice

Sari D. Okzelia[1,2], Satrialdi[1], Sjaikhurrizal E. Muttaqien[3], Boky J. Tuasikal[4], Diky Mudhakir[1]*

[1]*Department of Pharmaceutics, School of Pharmacy, Institut Teknologi Bandung (ITB), Jl. Ganesha No. 10, Bandung, 40132, Indonesia*
[2]*Department of Pharmacy, Faculty of Health and Pharmacy, Universitas Bani Saleh, Jl. R.A. Kartini No. 66, Bekasi, 17113, Indonesia*
[3]*Research Center for Vaccine and Drugs, National Research and Innovation Agency (BRIN), LAPTIAB 1, PUSPIPTEK, Tangerang Selatan, 15314, Indonesia*
[4]*Research Organization for Nuclear Energy, National Research and Innovation Agency (BRIN), KST B.J. Habibie Serpong, PUSPIPTEK, Tangerang Selatan, 15314, Indonesia*

ARTICLE INFO

Article history:
Received 07 June 2025
Revised 04 July 2025
Accepted 13 July 2025
Published online 01 September 2025

ABSTRACT

Delivering therapeutics to the brain is restricted by the blood-brain barrier (BBB). The intranasal route offers a non-invasive alternative to bypass the BBB, but its effectiveness is limited by rapid mucociliary clearance. To overcome this limitation, this study aimed to develop and characterize mucoadhesive thiolated chitosan (TCs) nanoparticles designed to prolong nasal residence time and facilitate nose-to-brain transport. Thiolated chitosan was synthesized, and its chemical modification was confirmed using Fourier-transform infrared spectroscopy (FTIR) and proton nuclear magnetic resonance (^{1}H-NMR). Nanoparticles from both TCs and unmodified chitosan (Cs) were then prepared by ionic gelation, incorporating Nile blue (NB) as a fluorescent probe. The synthesized TCs polymer showed a high degree of thiolation (491.38 ± 5.25 µmol/g). The resulting TCs nanoparticles had a mean particle size of 177.27 ± 4.14 nm, smaller than the Cs nanoparticles (229.03 ± 14.73 nm), with excellent entrapment efficiencies of 93.80% and 94.07%, respectively. *In vivo* biodistribution studies in male BALB/c mice revealed a prolonged nasal residence time of up to 6 hours for the TCs nanoparticles. Subsequent *ex vivo* analysis confirmed significantly higher accumulation of TCs nanoparticles in the nasal cavity compared to their Cs counterparts at 2 hours post-administration. Crucially, fluorescent signals originating from the TCs nanoparticle formulation were successfully detected in the brain. These findings demonstrate that thiolated chitosan nanoparticles are a potent mucoadhesive platform. By significantly increasing nasal residence time, this formulation enhances direct nose-to-brain delivery, presenting a promising strategy for transporting therapeutics to the central nervous system.

Keywords: Mucoadhesive polymer nanoparticles, *in vivo* study, *ex vivo* study, Brain targeting.

Introduction

The prevalence of debilitating central nervous system (CNS) disorders is rising steadily as the global population ages, creating an urgent need for effective therapies. However, treating CNS conditions such as Alzheimer's disease, Parkinson's disease, autoimmune dysfunction, and multiple sclerosis remains a formidable challenge. This difficulty stems primarily from the blood–brain barrier (BBB), a highly selective physiological shield that prevents most drugs from reaching the brain. The BBB blocks approximately 98% of small-molecule drugs and nearly 100% of macromolecules from entering the CNS, rendering many otherwise promising therapies ineffective for neurological applications.[1,2] Consequently, conventional administration routes, such as oral or intravenous injection, are largely ineffective for CNS targets due to the blocking effect of the BBB. This necessitates the development of alternative strategies that can deliver therapeutics to the brain efficiently and non-invasively.

*Corresponding author. Email: mudhakir@itb.ac.id
Tel: +6281321024600

Citation: Okzelia SD, Satrialdi, Muttaqien SE, Tuasikal BJ, Mudhakir D. Thiolated Chitosan Nanoparticles as a Promising Mucoadhesive Polymer in a Nose-to-Brain Delivery System: A Biodistribution Study in Mice. Trop J Nat Prod Res. 2025; 9(8): 3794 – 3801 https://doi.org/10.26538/tjnpr/v9i8.39

Official Journal of Natural Product Research Group, Faculty of Pharmacy, University of Benin, Benin City, Nigeria

The nose-to-brain (N2B) delivery route has emerged as a promising alternative, as it offers a direct pathway to the CNS along the olfactory and trigeminal nerves, thereby bypassing the BBB.[3] Furthermore, this approach avoids hepatic first-pass metabolism and minimizes systemic exposure. Despite its promise, the clinical translation of N2B delivery is hindered by rapid mucociliary clearance, which expels formulations from the nasal cavity within minutes.[4] This short residence time drastically limits the window for drug absorption. To overcome this, mucoadhesive polymers are widely employed to prolong contact time with the nasal mucosa. Chitosan (Cs), a biocompatible and biodegradable polysaccharide classified as Generally Recognized as Safe (GRAS), is a popular choice due to the electrostatic interaction between its positive charge and the negatively charged mucosal surface.[5] However, this interaction is non-covalent and can be relatively weak, leading to suboptimal residence times under physiological conditions. The strategy of improving formulation performance through enhanced mucoadhesion is central to advancing intranasal drug delivery. In this context, the chemical modification of chitosan via thiolation is a well-established method to significantly boost mucoadhesive strength. Unlike the electrostatic interactions of standard chitosan, thiolated chitosan (TCs) forms strong, covalent disulfide bonds with glycoproteins in the mucus layer, which is hypothesized to prolong nasal residence time and increase the opportunity for drug transport to the brain.[6,7] However, there is a lack of direct *in vivo* research that visualizes and quantifies the retention advantage of TCs nanoparticles over standard Cs nanoparticles and correlates this with subsequent brain accumulation. This knowledge gap limits a clear understanding of the true therapeutic potential that thiolation offers for N2B delivery systems. Therefore, the primary aim of this research was to develop and characterize a TCs nanoparticle system and to quantitatively evaluate its potential for enhanced nasal retention and

brain accumulation. To achieve this, we first optimized the synthesis of TC to achieve a high degree of thiolation. We then formulated nanoparticles from both TCs and unmodified Cs, loading them with a fluorescent dye (Nile Blue). The relevance of using this dual-formulation approach is to provide a direct, controlled comparison. Finally, using an *In Vivo* Imaging System (IVIS), we directly visualized and quantified the biodistribution of the nanoparticles over time. By providing novel, quantitative evidence of prolonged nasal residence and subsequent brain accumulation, this study provides a strong rationale for the continued development of TCs nanoparticles as a superior drug carrier for CNS-targeted therapies.

Materials and Methods

Reagents and Chemicals

Thioglycolic acid (≥99%, reagent grade; Cat. No. 528056), chitosan (low molecular weight, 75–85% deacetylated, MW ~50–190 kDa; Cat. No. 448869), N-(3-dimethylaminopropyl)-N′-ethylcarbodiimide hydrochloride (EDAC, ≥98%, molecular biology grade; Cat. No. E7750), sodium hydroxide (≥97%, reagent grade; Cat. No. 655104), hydrochloric acid (36.5–38%, BioReagent grade; Cat. No. H1758), potassium bromide (≥99%, Trace metals basis; Cat. No. 221864), Ellman's reagent (5,5′-Dithiobis(2-nitrobenzoic acid), DTNB, ≥99%, ReagentPlus®; Cat. No. D218200), sodium dihydrogen phosphate (NaH_2PO_4, ≥98%, ACS reagent; Cat. No. S9638), disodium hydrogen phosphate (Na_2HPO_4, ≥99%, ACS reagent; Cat. No. S0876), glacial acetic acid (≥99.7%, analytical grade), sodium tripolyphosphate (STPP, ≥85%, technical grade; Cat. No. 238503), and Nile blue chloride (dye content 85%, microscopy grade; Cat. No. 222550) were purchased from Sigma-Aldrich (St. Louis, MO, USA). Sodium chloride (NaCl, ≥99%, analytical grade) was obtained from Himedia (Mumbai, India), and dialysis tubing with a molecular weight cut-off (MWCO) of 12–14 kDa was procured from Carolina Biological Supply Company (Burlington, NC, USA).

Animals

Healthy male BALB/c mice (weight: 20 ± 2 g; age: 5–7 weeks) were used in this study. The animals were housed under standard laboratory conditions: a 12-hour light/dark cycle, constant temperature (23 ± 3°C), and relative humidity (50 ± 10%), with unrestricted access to standard food and water. All animal procedures were conducted in strict accordance with ethical standards and were approved by the Ethics Committee of the National Research and Innovation Agency (BRIN), Indonesia. Ethical Clearance Approval No: 245/KE.02/SK/10/2024.

Synthesis of TCs

The synthesis of TCs was performed using a previously reported method,[8] with some modifications. Briefly, 1 mL of TGA (1% w/v) was added to a chitosan polymer solution (1% v/v). Subsequently, EDAC was added to the solution, and the pH of the mixture was adjusted to 5.0 with 5 M NaOH. The resulting mixture was incubated for 4 hours at room temperature (20-25 ºC) with continuous stirring at 700 rpm using a magnetic stirrer. Following this, dialysis was performed using a cellulose dialysis bag (12-14 kDa) against 5 mM HCl, followed by two rounds against 5 mM HCl containing 1% w/v NaCl, and finally against 1 mM HCl. The dialysis product was then removed, lyophilized using FreeZone 2.5 Liter Benchtop Freeze Dryer (Labconco, Kansas City, MO, USA), and stored at 4 °C for further use.

Characterizations of TCs

Cs and TCs were characterized using FTIR and ^{1}H-NMR spectroscopy. For the FTIR analysis, the sample was mixed with KBr at a 1:100 ratio and compressed into a pellet.[9] The FTIR spectrum was recorded in the 4000–400 cm^{-1} wavenumber range using a Jasco FT/IR-4200 type A spectrometer (Jasco Corporation, Tokyo, Japan). For the ^{1}H-NMR analysis, the TCs sample was dissolved in deuterium oxide (D_2O). The ^{1}H-NMR spectrum was measured using a Bruker NMR spectrometer (Bruker Corporation, Billerica, MA, USA).

Determination of Thiol Contents

The quantity of thiol groups was determined spectrophotometrically using Ellman's reagent, following a previously reported procedure.[10] Briefly, 2 mg of TCs were dissolved in 1 mL of deionized water to prepare a sample solution. In parallel, a solution of Ellman's reagent was prepared by dissolving 2 mg of the reagent in 1 mL of 0.1 M phosphate buffer solution (PBS, pH 8.0). For the assay, 100 µL of the TCs sample solution, 900 µL of 0.5 M PBS (pH 8.0), and 1000 µL of the Ellman's solution were added to a test tube. The mixture was incubated in the dark for 15 minutes at room temperature (20-25 ºC), after which its absorbance was measured at a wavelength of 412 nm using a UV-Vis spectrophotometer (Thermo Scientific, Waltham, MA, USA). A standard calibration curve was prepared using TGA over a concentration range of 0.00–0.40 mM.

Preparation of Cs and TCs Nanoparticles

TCs and unmodified Cs nanoparticles were prepared via an ionic gelation process, following a previously reported procedure.[11] Stock solutions of Cs and TCs were prepared at a concentration of 1.40 mg/mL in a 1% v/v acetic acid solvent. The pH of each solution was adjusted to 4.7 with 5 M NaOH, and the solutions were then filtered through a 0.22 µm syringe filter. A separate solution of sodium tripolyphosphate (STPP) was prepared at a concentration of 1.40 mg/mL in deionized water and was also filtered through a 0.22 µm syringe filter. To synthesize the nanoparticles, 712 µL of either the Cs or TCs solution was mixed with 50 µL of deionized water and stirred at 700 rpm for 1 minute using a magnetic stirrer. Subsequently, 238 µL of the STPP solution was added dropwise to the mixture while stirring continued for an additional 2 minutes. The resulting nanoparticle suspension was centrifuged for 20 minutes at 13,000 rpm using a microcentrifuge (Eppendorf Minispin, Hamburg, Germany). The supernatant was discarded, and the nanoparticle pellet was redispersed in 100 µL of deionized water. The final suspension was collected in a clean glass vial, and the total volume was adjusted to 1000 µL with deionized water. Finally, the nanoparticle suspension was sonicated six times for 10 seconds each at 70% amplitude using an ultrasonication probe.

Preparation of Nile Blue-labeled Cs and TCs Nanoparticles

Nile Blue-labeled TCs and unmodified Cs nanoparticles were prepared via an ionic gelation process, following a previously reported procedure.[11] First, stock solutions of the polymers (Cs and TCs) were prepared at a concentration of 1.40 mg/mL in a 1% v/v acetic acid solvent. A separate stock solution of Nile Blue was prepared at a concentration of 10 mg/mL in ethanol. A solution of sodium tripolyphosphate (STPP) was also prepared at a concentration of 1.40 mg/mL in deionized water. All solutions were filtered through a 0.22 µm syringe filter prior to use. To synthesize the fluorescent nanoparticles, 712 µL of a polymer solution was placed in a vial. To this, 50 µL of the Nile Blue stock solution was added, corresponding to a dye-to-polymer weight ratio of approximately 50 %. The mixture was briefly vortexed and stirred at 700 rpm for 1 minute using a magnetic stirrer. Subsequently, 238 µL of the STPP solution was added dropwise to the fluorescent polymer solution while stirring continued for an additional 2 minutes. The resulting nanoparticle suspension was centrifuged for 20 minutes at 13,000 rpm using a microcentrifuge (Eppendorf Minispin, Hamburg, Germany). The supernatant was discarded, and the nanoparticle pellet was redispersed in 100 µL of deionized water. The final suspension was collected in a clean glass vial, and the total volume was adjusted to 1000 µL with deionized water. Finally, the nanoparticle suspension was sonicated six times for 10 seconds each at 70% amplitude using an ultrasonication probe to ensure homogeneity.

Determination of Entrapment Efficiency and Loading Capacity

To quantify the amount of non-encapsulated Nile Blue, the supernatant was collected after the centrifugation step of the nanoparticle preparation. This supernatant was then diluted 100-fold with deionized water, and its absorbance was measured at a wavelength of 639 nm using a UV-Vis spectrophotometer (Thermo Scientific, Waltham, MA, USA). The concentration of free dye in the supernatant was determined from a standard calibration curve. The entrapment efficiency (EE) and loading capacity (LC) were subsequently calculated using the following equations (equation 1 and 2):[12]

$$\text{Entrapment Efficiency (\%)} = \frac{\text{Initial amount of NB} - \text{amount of NB unentrapped}}{\text{Initial amount of NB}} \text{x100} = \text{Equation 1}$$

$$\text{Loading Capacity (\%)} = \frac{\text{Initial amount of NB} - \text{amount of NB unentrapped}}{\text{Amount of Cs or TCs added}} \text{x100} = \text{Equation 2}$$

Determination of Particle Size, Polydispersity Index, and Zeta Potential
The particle size, polydispersity index (PDI), and zeta potential of all nanoparticle formulations (unlabeled and Nile Blue-labeled Cs and TCs) were analyzed by Dynamic Light Scattering (DLS). Measurements were performed using a DelsaMax PRO particle size and zeta potential analyzer (Beckman Coulter, West Sacramento, CA, USA).

In Vivo Biodistribution Study
The *in vivo* biodistribution of the nanoparticles following intranasal administration was evaluated using Nile Blue (NB)-labeled formulations. Mice were divided into three groups and were intranasally administered one of the following: 0.9% NaCl saline (control), Cs-NB nanoparticles, or TCs-NB nanoparticles, at a volume of 40 µL per mouse.[13] Prior to and during imaging, each animal was anesthetized with 5% isoflurane. The biodistribution was monitored by capturing whole-body fluorescent images at several time points post-administration (0.5, 1, 2, 3, 4, 6, and 24 h) using an *in vivo* imaging system (IVIS Spectrum, Revvity, Hopkinton, MA, USA).

Ex vivo Biodistribution Study
To visualize organ-specific distribution, separate cohorts of mice were used for *ex vivo* analysis. The experimental groups were administered treatments intranasally as described in the *in vivo* study: 0.9% NaCl saline (control), Cs-NB nanoparticles, and TCs-NB nanoparticles, each at a volume of 40 µL per mouse. The mice (n=3 per group per time point) were sacrificed after 0.5, 2, and 3 h post-administration. The brain (including the olfactory bulb) and the nasal cavity (a 0.5 cm length section) were immediately harvested, frozen, and subsequently imaged using the IVIS Spectrum to determine the *ex vivo* fluorescence intensity.[14,15]

Statistical Analysis
The results were presented as the mean ± standard deviation of three measurement replicates. Student's t-test or one-way ANOVA was used if applicable, and the value of $p < 0.10$ was considered the significance level. All analyses were performed with SPSS Statistics (Version 25).

Results and Discussion

Synthesis of TCs
Thiolated chitosan (TCs) was successfully synthesized as a white, amorphous, and fibrous solid following lyophilization of the purified polymer solution. The appearance of the final product is consistent with previous reports on similar thiomers.[16,17] The synthesis (**Figure 1**) proceeds via an EDAC-mediated amide bond formation between the primary amino group at the C-2 position of chitosan and the carboxyl group of thioglycolic acid (TGA).
The success of this synthesis and the purity of the final product were ensured by a carefully controlled reaction and purification strategy. The reaction was conducted at pH 5 for 4 hours, creating an optimal environment for the EDAC coupling mechanism, which involves the formation of a reactive O-acylisourea intermediate.[18] Subsequently, a rigorous multi-step dialysis was critical for purification. This protocol featured a salt wash (1% NaCl in 5 mM HCl) to disrupt any lingering ionic interactions between the cationic polymer backbone and anionic TGA. The process concluded with dialysis against 1 mM HCl to condition the polymer to a final pH of approximately 4. This terminal pH is essential, as it maximizes polymer stability by minimizing the concentration of reactive thiolate anions, thereby preventing undesirable oxidative disulfide cross-linking.[18]

Characterizations of TCs
The successful covalent conjugation of TGA onto the chitosan backbone was definitively confirmed by FTIR and ^{1}H-NMR spectroscopy. The FTIR spectrum of the synthesized TCs (**Figure 2**) provides key points of evidence when comparing the spectra of Cs, TGA, and TCs.

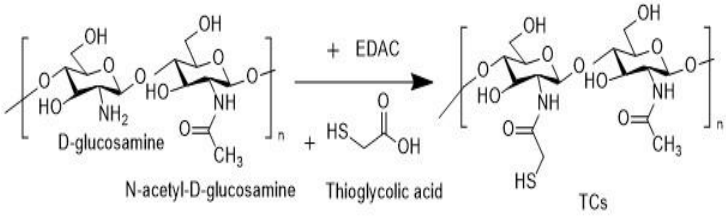

Figure 1: Synthesis reaction of TCs

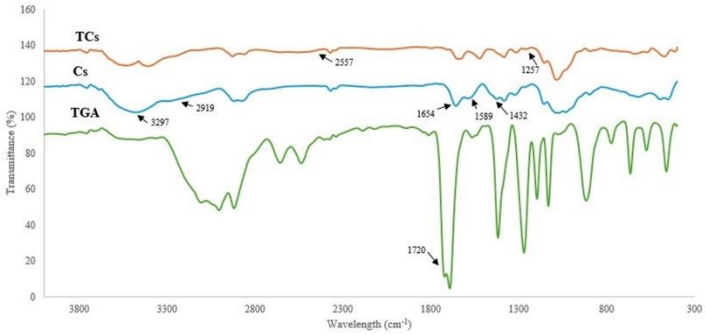

Figure 2: FTIR spectrum of TCs, Cs, and TGA

A sharp absorption peak at 1720 cm^{-1} is observed in the TGA spectrum, corresponding to the stretching C=O bond of the carboxylic acid group in TGA. This peak disappears after TGA reacts with Cs, indicating that TGA has successfully conjugated with Cs through a covalent bond.[19] On the other hand, the peaks at 1654 cm^{-1} and 1589 cm^{-1} in Cs, respectively, indicate the absorption of the amide I bond (O=C-NH) and the bending deformation of the -NH bond. Additionally, in the Cs spectrum, stretching vibrations of -NH and -OH are observed at 3297 cm^{-1} and 2919 cm^{-1}, respectively, as well as the bending of the -CH bond at 1423 cm^{-1}. Thiolation of Cs to form TCs was confirmed by the characteristic absorption of the sulfhydryl group (-SH) at 2557 cm^{-1}.
The FTIR spectrum results in this study are consistent with research by Luo et al.[10] and Abbas et al.,[20] who respectively found that the sulfhydryl group in synthesized thiolated chitosan appeared at wavenumbers 2500-2560 cm^{-1} and 2122 cm^{-1}.[10,20] Furthermore, the characteristic absorption of the C-SH stretching was found at 1257 cm^{-1} in TCs but not in Cs. This is consistent with the previous study which found the C-SH stretching at 1220 cm^{-1}.[15] Complementary analysis by ^{1}H-NMR spectroscopy (**Figure 3**) corroborated these findings, displaying a distinct singlet at 2.09 ppm assigned to the methylene protons adjacent to the newly introduced sulfhydryl group, providing conclusive evidence of successful thiolation.[10]

Determination of Thiol Contents
The degree of thiolation in the TCs polymer was quantified using a visible spectrophotometry method employing 5,5′-dithiobis(2-nitrobenzoic acid), commonly known as Ellman's reagent. The assay's mechanism relies on a rapid thiol-disulfide exchange, where the reagent reacts with free thiols to release a distinctly colored chromophore that can be measured to determine thiol content.[21]
Given that DTNB is highly sensitive and specific for this exchange reaction at neutral pH, it served as a reliable tool for our optimization studies.[17] The initial investigation revealed that the molar ratio of chitosan: EDAC:TGA did not significantly impact the final thiol

content. Consequently, a resource-efficient 1:1:1 ratio was selected and used for the subsequent optimization of the EDAC concentration. This next phase of optimization showed that a concentration of 100 mM EDAC was optimal, yielding a maximal thiol content of 491.38±5.25 µmol/g. This result is notably higher than the 261.8 µmol/g reported in a comparable study by Khatoon et al.,[8] highlighting the efficacy of our approach.

While factors such as pH and reaction time can influence thiol quantification,[22] their effects were minimized in this study by using a robust standard calibration curve method. To generate this curve, TGA was used as the standard in a concentration range of 0.00–0.40 mM. The number of thiol groups was then calculated using the resulting linear regression equation, y = 0.7272x + 0.5584, which showed excellent linearity ($R^2 = 0.9982$). The TGA standard calibration curve is presented in **Figure 4**.

The rationale for this two-step optimization was to systematically isolate the most critical reaction parameters. The initial comparison of Cs and TGA amounts was conducted as they are the primary reactants (with Cs acting as the polymer backbone and TGA as the thiolation agent). The results of this initial screening are shown in **Figure 5**.

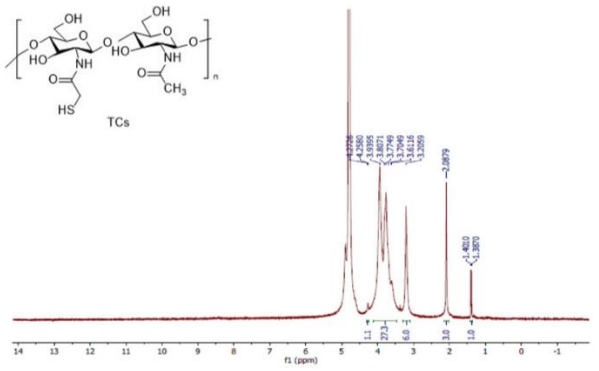

Figure 3: ^{1}H-NMR spectra of TCs

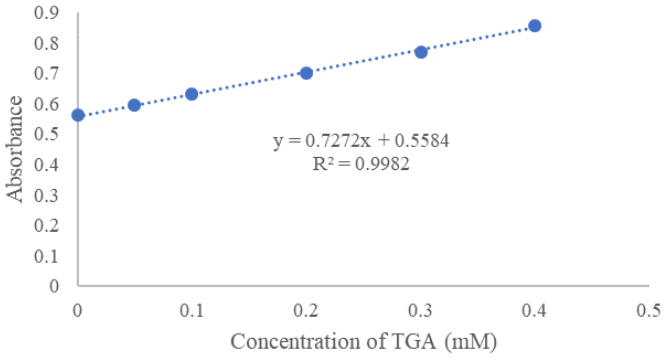

Figure 4: Calibration curve of TGA standards

The finding that the reactant amounts were not the limiting factor is consistent with the reaction's 1:1:1 stoichiometry (**Figure 1**). Therefore, a TGA:EDAC:Cs ratio of 1:1:1 was confidently used for all further experiments. The focus then shifted to the coupling agent, EDAC, as its role in activating the TGA carboxyl group is paramount to the success of the thiolation. This activation proceeds via an active O-acylisourea intermediate, which is then susceptible to nucleophilic attack by the primary amines on the chitosan backbone, forming the desired amide bond and releasing a soluble urea byproduct.[23]

The subsequent optimization of EDAC concentration over a 50–125 mM range confirmed its critical importance. The results demonstrated that 100 mM was the optimal concentration, yielding the previously noted maximum thiol content of 491.38 ± 5.25 µmol/g. At sub-optimal concentrations (e.g., 50 and 75 mM), it is likely that not all TGA carboxylate groups were activated. Conversely, at supra-optimal concentrations (e.g., 125 mM), the decrease in efficiency can be attributed to the known instability of the O-acylisourea intermediate in aqueous solution, which can hydrolyze before reacting.[24]

Finally, to provide definitive validation that 100 mM EDAC was the optimal condition, a concluding evaluation was performed. The TGA:Cs ratio was varied once more (1:2 and 2:1) while holding the EDAC concentration at 100 mM. This confirmed that the reactant ratio had a negligible effect on the thiol content. Thus, under the fully optimized conditions of 100 mM EDAC with a 1:1:1 reactant ratio, the synthesis yielded 41.63 ± 3.12% of the TCs polymer with a maximum solid content of 6.55 ± 0.07%. The comprehensive optimization results are summarized in **Figure 6**.

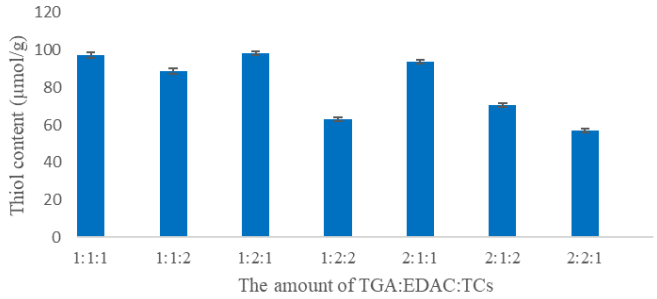

Figure 5: The optimization results of the comparison of the amounts of TGA, EDAC, and Cs using 50 mM EDC

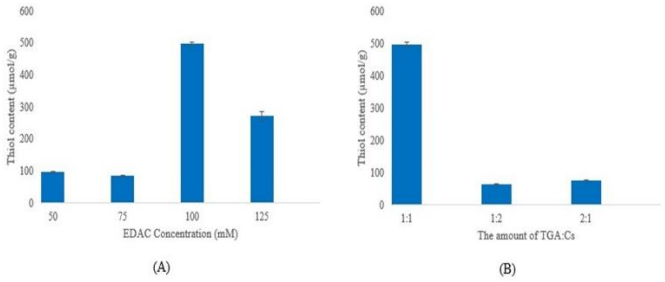

Figure 6: The optimization results of the various EDAC concentrations (A); and the comparison of the amounts of TGA:Cs using 100 mM EDAC

Preparation and Characterizations of Nanoparticles

TCs nanoparticles were successfully prepared using the ionic gelation method, with STPP solution serving as a cross-linking agent. The concentration of the TCs nanoparticle core obtained from this procedure was 1 mg/mL. The characterization results are summarized in **Table 1.** Both Cs and TCs nanoparticles were successfully synthesized, exhibiting particle sizes of 193.70 ± 5.05 nm and 171.03 ± 4.96 nm, respectively. Nile Blue (NB) was effectively encapsulated within Cs and TCs nanoparticles, resulting in particle sizes of 229.03 ± 14.73 nm and 177.27 ± 4.14 nm, respectively.

Notably, TCs and TCs-NB nanoparticles exhibited smaller sizes than their Cs and Cs-NB counterparts at the same concentration. This reduction in size is attributed to the incorporation of thiol groups in TCs, which induce structural changes in the polymer network. These structural modifications influence the size of the resulting aggregates or particles.[25]

Table 1: Characteristics of nanoparticles

Characteristics	Type of Nanoparticles			
	Cs	TCs	Cs-NB	TCs-NB
Particle size (nm)	193.70±5.05	171.03±4.96	229.03±14.73	177.27±4.14
Polydispersity index	0.290±0.041	0.254±0.119	0.268±0.062	0.254±0.057
Zeta potential (mV)	37.87±1.20	31.35±1.29	39.48±0.56	35.73±0.80
Entrapment efficiency (%)	*N/A	*N/A	94.07±0.07	93.80±0.05
Loading capacity (%)	*N/A	*N/A	47.18±0.04	47.05±0.02

*N/A: not applicable

The polydispersity index (PDI) reflects the uniformity of the nanoparticle population. In this study, PDI values below 0.5 indicate a monodisperse system with minimal size variability and negligible aggregation.[26] Zeta potential measurements showed values of 37.87 ± 1.20 mV for Cs nanoparticles and 31.35 ± 1.29 mV for TCs nanoparticles. The positive surface charge of Cs nanoparticles is attributed to the presence of free amine groups. In contrast, the reduced positive charge in TCs nanoparticles is due to interactions between amine groups and negatively charged thiol groups.

Encapsulation of Nile Blue further influenced the surface charge. Cs-NB nanoparticles exhibited an increased zeta potential of 39.48 ± 0.56 mV, reflecting the incorporation of the positively charged dye. Meanwhile, TCs-NB nanoparticles demonstrated a slightly reduced zeta potential of 35.73 ± 0.80 mV, likely due to the presence of thiol groups in the TCs matrix. A zeta potential above ±30 mV is generally considered sufficient to ensure colloidal stability.[11]

In this study, the EE values for Cs-NB and TCs-NB nanoparticles were determined to be 94.07 ± 0.086% and 93.80 ± 0.047%, respectively. These high EE values indicate robust encapsulation efficiency for both nanoparticle systems, which align with principle that hydrophilic polymers demonstrate superior entrapment of hydrophilic drugs and dyes . Similarly, the LC values were 47.18 ± 0.043% for Cs-NB and 47.05 ± 0.024% for TCs-NB, reflecting substantial loading potential. These results highlight the effectiveness of the nanoparticle formulations in achieving high encapsulation and loading efficiencies for Nile blue dye for robust imaging applications.

In Vivo Biodistribution Study

A critical prerequisite for successful nose-to-brain drug delivery is the ability of a carrier system to overcome the rapid mucociliary clearance mechanisms within the nasal cavity. We therefore hypothesized that the TCs nanoparticles would exhibit enhanced mucoadhesion and, consequently, a prolonged nasal residence time compared to unmodified Cs nanoparticles. To investigate this, an *in vivo* biodistribution study was conducted using Nile Blue as a fluorescent probe.

Qualitative imaging results first revealed a striking difference in retention between the two formulations (**Figure 7**). While the unmodified Cs nanoparticles were largely cleared from the nasal cavity within two hours of administration, the TCs nanoparticles were clearly retained, with a strong fluorescent signal still detectable six hours post-administration. This visual finding was corroborated by a quantitative analysis of the average radiant efficiency over the study period (**Figure 8**).

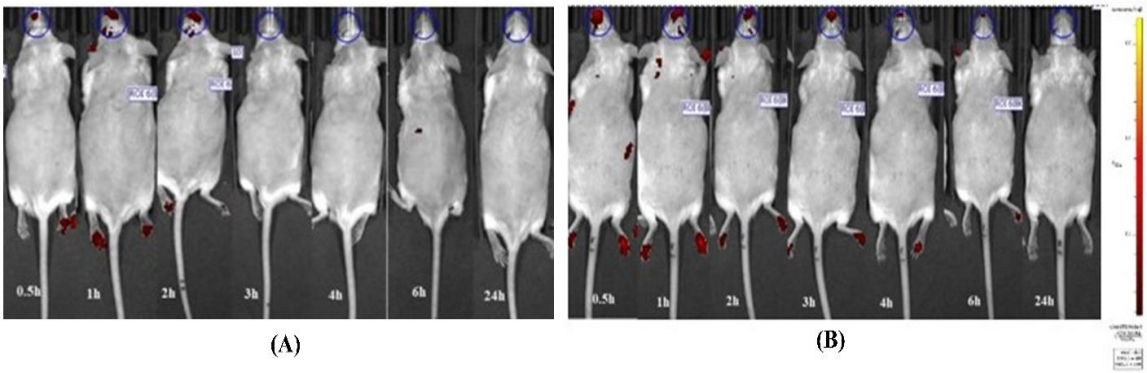

Figure 7: In vivo bioimaging of the nasal cavity at 0.5h, 1h, 2h, 3h, 4h, 6h, and 24h after intranasal administration of Cs (A) and TCs (B) nanoparticles

The data revealed a statistically significant difference between the two groups, confirming that the TCs nanoparticles maintained a substantially higher concentration in the nasal region over time.

The superior retention of the TCs formulation is directly attributed to the well-established mucoadhesive properties conferred by the thiol groups. These functional groups are known to form covalent disulfide bonds with the cysteine-rich glycoproteins present in the nasal mucus layer.[19,27] This interaction effectively anchors the TCs nanoparticles to the mucosal surface, significantly arresting their clearance. Collectively, these findings demonstrate that thiolation is a highly effective strategy for enhancing the nasal residence time, making the TCs platform a far more promising carrier for intranasal administration, representing a critical step toward the ultimate goal of brain-targeted drug delivery.

Ex Vivo Biodistribution Study

To further elucidate and quantify the nanoparticle biodistribution observed *in vivo*, an *ex vivo* analysis of harvested organs was performed at 0.5, 2, and 3 hours post-administration. The results from the excised nasal cavity and brain tissues provided a more detailed assessment of nanoparticle accumulation and retention over time (**Figure 9**). The primary findings from this study relate to the retention of nanoparticles within the nasal cavity. The *ex vivo* imaging corroborated the *in vivo* data, confirming that TCs nanoparticles exhibited a significantly higher fluorescence intensity compared to unmodified Cs nanoparticles at all time points. This quantitative analysis, presented in **Figure 10**, underscores the superior mucoadhesive properties imparted by thiolation. Notably, the accumulation of TCs nanoparticles peaked at the 2-hour mark, showing a greater signal intensity than at the 0.5 and 3-hour intervals.

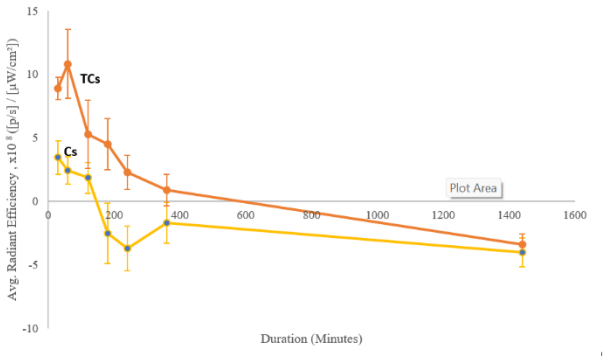

Figure 8: In vivo average radiant efficiency of Cs and TCs nanoparticles in nasal cavity after intranasal administration

This suggests an optimal residence time window, which can be attributed to the dynamic process of covalent disulfide bond formation between the thiol groups on the TCs and the cysteine-rich domains of mucin glycoproteins in the nasal mucosa. This strong, covalent interaction likely accounts for the prolonged retention of TCs nanoparticles compared to the primarily electrostatic, and thus weaker, interaction of unmodified Cs nanoparticles. Regarding brain delivery, the fluorescence signals detected from the brain tissue were low for both formulations. However, the signals were consistently above background levels, confirming that a small fraction of both Cs and TCs nanoparticles was capable of reaching the brain following intranasal administration. While the difference in brain accumulation between the two formulations was not as pronounced as in the nasal cavity, the TCs nanoparticles displayed a slightly higher trend in signal intensity, aligning with the hypothesis that increased nasal residence time can lead to enhanced nose-to-brain transport.[28]

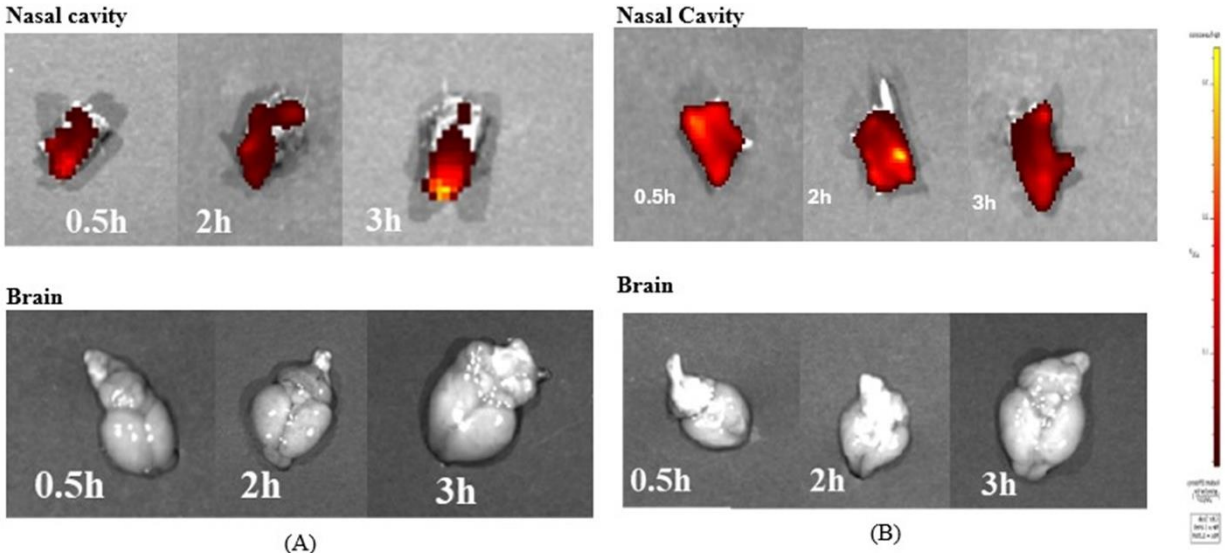

Figure 9: Ex vivo bioimaging of the nasal cavity and brain at 0.5h, 2h, and 3h after intranasal administration of Cs (A) and TCs (B) nanoparticles

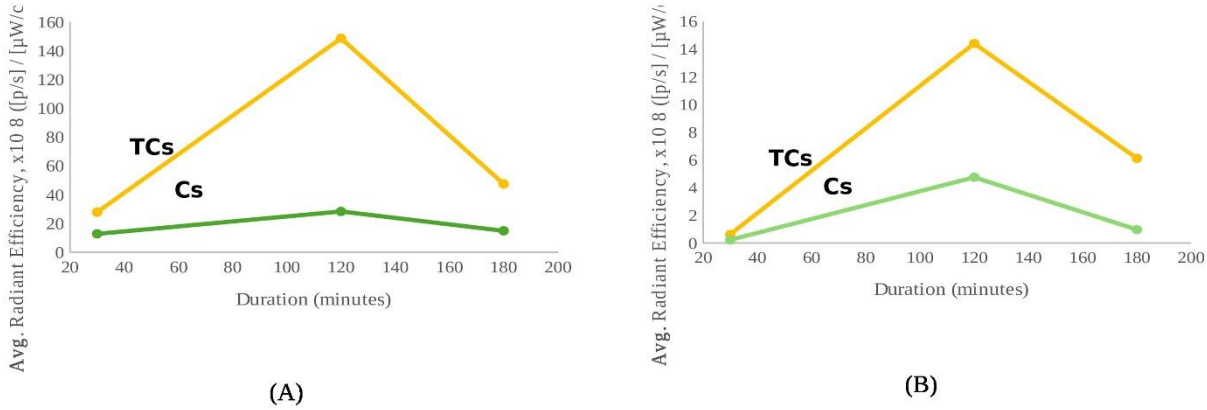

Figure 10: Ex vivo average radiant efficiency of Cs and TCs nanoparticles in nasal cavity (A) and brain (B) after intranasal administration

Collectively, these *ex vivo* results strongly support the potential of TCs nanoparticles as a superior mucoadhesive carrier for intranasal drug delivery. By significantly enhancing residence time in the nasal cavity, the thiolated formulation creates a more favorable condition for subsequent transport to the central nervous system. Future work will therefore focus on optimizing TCs nanoparticle formulations to leverage this enhanced nasal retention for significantly improved brain accumulation and therapeutic efficacy.

Conclusion

The successful synthesis of TCs has led to significant advancements in enhancing mucoadhesive properties in the nasal cavity for nose-to-brain delivery. The *in vivo* biodistribution study revealed that TCs nanoparticles had a residence time of 6 hours in the nasal cavity, whereas Cs nanoparticles had only 2 hours. Furthermore, the *ex vivo* biodistribution study demonstrated that TCs nanoparticles accumulated in the nasal cavity at a much higher amount than Cs nanoparticles at the 2-hour mark. Signals were also detected in the mouse brain. These findings emphasize the potential of TCs nanoparticles as mucoadhesive polymers for delivering drugs to the brain by prolonging their residence time in the nasal mucosal glands. Future studies will focus on developing TCs nanoparticle formulations to enhance brain accumulation further.

Conflict of Interest

The authors declare no conflicts of interest.

Authors' Declaration

The authors hereby declare that the work presented in this article is original and that any liability for claims relating to the content of this article will be borne by them.

Acknowledgments

The authors acknowledge the facilities, scientific and technical support from *In Vivo* Imaging Laboratory, National Research and Innovation Agency (BRIN) for In *Vivo* Imaging System (IVIS) spectrum analysis. We sincerely thank Prasetya Widodo, S.T., M.Si. from the Directorate of Laboratory Management, Research Facilities, and Science and Technology Park, BRIN, for assisting us during the *in vivo* imaging study. We are also profoundly grateful to the Ministry of Education, Culture, Research, and Technology, Directorate General of Higher Education, Research, and Technology of Indonesia for their generous research grant (Contract No. 036/E5/PG.02.00.PL/2024).

References

1. Jiao Y, Yang L, Wang R, Song G, Fu J, Wang J, Gao N, Wang H. Drug delivery across the blood-brain barrier: A new strategy for the treatment of neurological diseases. Pharmaceutics. 2024; 16(12):1611.
2. Crowe TP, Greenlee MHW, Kanthasamy AG, Hsu WH. Mechanism of intranasal drug delivery directly to the brain. Life Sci. 2018; 195:44-52.
3. Samaridou E, Alonso MJ. Nose-to-brain peptide delivery – The potential of nanotechnology. Bioorg Med Chem. 2018; 26(10):2888-2905.
4. Jeong SH, Jang JH, Lee YB. Drug delivery to the brain via the nasal route of administration: exploration of key targets and major consideration factors. J Pharm Investig. 2023; 53:119-152.
5. Zahir-Jouzdani F, Wolf JD, Atyabi F, Bernkop-Schnürch A. In situ gelling and mucoadhesive polymers: why do they need each other? Expert Opin Drug Deliv. 2018; 15(10):1007-1019.
6. Yu S, Xu X, Feng J, Liu M, Hu K. Chitosan and chitosan coating nanoparticles for the treatment of brain disease. Int J Pharm. 2019; 560:282-293.
7. Sunena, Singh K, Mishra DN. Nose to brain delivery of galantamine loaded nanoparticles: in vivo pharmacodynamic and biochemical study in mice. Curr Drug Deliv. 2019; 16(1):51-58.
8. Khatoon M, Sohail MF, Shahnaz G, Rehman F, Fakhar-ud-Din, Rehman A, Ullah N, Amin U, Khan GM, Shah KU. Development and evaluation of optimized thiolated chitosan proniosome containing duloxetine for intranasal delivery. AAPS PharmSciTech. 2019; 20(8):288.
9. Sadaqa E, Kurniawan F, Mudhakir D. Sodium oleate functionalized simvastatin liposomes: boosting endosomal escape and anticancer efficacy in triple negative breast cancer. Res Pharm Sci. 2025; 20(2):188-206.
10. Luo Q, Han Q, Wang Y, Zhang H, Fei Z, Wang Y. Thiolated chitosan: Synthesis, gelling and antibacterial capability. Int J Biol Macromol. 2019; 139:521-530.
11. Sadaqa E, Utami RA, Mudhakir D. In vitro cytotoxic and genotoxic effects of *Phyllanthus niruri* extract loaded chitosan nanoparticles in TM4 cells and their influence on spermatogenesis. Pharmacia. 2024; 71(1):1-14.
12. Mudhakir D, Sadaqa E, Permana Z, Mumtazah JE, Zefrina NF, Xeliem JN, Hanum LF, Kurniati NF. Dual-functionalized mesoporous silica nanoparticles for celecoxib delivery: amine grafting and imidazolyl PEI gatekeepers for enhanced loading and controlled release with reduced toxicity. Molecules. 2024; 29(15):3546.
13. Baek SH, Hwang EH, Hur GH, Lee YJ, Choe YS, Lee KH, Lee BC. Intranasal administration enhances size-dependent pulmonary phagocytic uptake of poly(lactic-co-glycolic acid) nanoparticles. EJNMMI Radiopharm Chem. 2024; 9(1):4.
14. Erdő F, Bors LA, Farkas D, Bajza Á, Gizurarson S. Evaluation of intranasal delivery route of drug administration for brain targeting. Brain Res Bull. 2018; 143:155-170.
15. Yang YL, Zhang XY, Wu SW, Zhang R, Zhou BL, Zhang XY, Tang L, Tian Y, Men K, Yang L. Enhanced nose-to-brain delivery of siRNA using hyaluronan-enveloped nanomicelles for glioma therapy. J Control Release. 2022; 342:66-80.
16. Inamdar NN, Mourya V. Thiolated chitosan preparation, properties, and applications. In: Kim SK, editor. Chitin and Chitosan Derivatives: Advances in Drug Discovery and Future Therapeutics. 1st ed. Boca Raton: CRC Press/Taylor and Francis; 2013. p. 121-145.
17. Kousar K, Naseer F, Abduh MS, Kakar S, Gul R, Anjum S, Ahmad T, Niazi MFK, Al-Harrasi A, Al-Rawahi A, Ali B. Green synthesis of hyaluronic acid coated, thiolated chitosan nanoparticles for CD44 targeted delivery and sustained release of Cisplatin in cervical carcinoma. Front Pharmacol. 2023; 14:1270278.
18. Arshad M, Sarwar HS, Sarfraz M, Jalil A, Bin Jardan YA, Farooq U, Sohail MF. Cholic acid-grafted thiolated chitosan-enveloped nanoliposomes for enhanced oral bioavailability of azathioprine: In vitro and in vivo evaluation. ACS Omega. 2024; 9:32807-32816.
19. Federer C, Kurpiers M, Bernkop-Schnürch A. Thiolated chitosans: A multi-talented class of polymers for various applications. Biomacromolecules. 2021; 22(1):24-56.
20. Abbas G, Rasul A, Fakhar-e-Alam M, Saadullah M, Muzammil S, Iqbal O, Atif M, Hanif M, Shah S, Ahmad S, Shafeeq S, Afzal M. Nanoparticles of thiolated chitosan for controlled delivery of moxifloxacin: In-vitro and in-vivo evaluation. J King Saud Univ Sci. 2022; 34(7):102218.
21. Zhu X, Su M, Tang S, Wang L, Liang X, Meng F, Hong Y, Xu Z. Synthesis of thiolated chitosan and preparation of nanoparticles with sodium alginate for ocular drug delivery. Mol Vis. 2012; 18:1973-1982.
22. Schmidt R, Logan MG, Patty S, Ferracane JL, Pfeifer CS, Kendall AJ. Thiol quantification using colorimetric thiol-disulfide exchange in nonaqueous solvents. ACS Omega. 2023; 8:9356-9363.
23. Khalid A, Sarwar HS, Sarfraz M, Sohail MF, Jalil A, Bin Jardan YA, Arshad R, Tahir I, Ahmad Z. Formulation and characterization of thiolated chitosan/polyvinyl acetate based microneedle patch for transdermal delivery of dydrogesterone. Saudi Pharm J. 2023; 31(5):669-677.

24. Chen X, Soria-Carrera H, Zozulia O, Boekhoven J. Suppressing catalyst poisoning in the carbodiimide-fueled reaction cycle. Chem Sci. 2023; 14(44):12653-12660.
25. Pratap-Singh A, Guo Y, Baldelli A, Singh A. Mercaptonicotinic acid activated thiolated chitosan (MNA-TG-chitosan) to enable peptide oral delivery by opening cell tight junctions and enhancing transepithelial transport. Sci Rep. 2023; 13(1):17343.
26. Sadaqa E, Satrialdi, Kurniawan F, Mudhakir D. Mechanistic insights into endosomal escape by sodium oleate-modified liposomes. Beilstein J Nanotechnol. 2024; 15:1667-1685.
27. Shahid N, Erum A, Zaman M, Iqbal MO, Riaz R, Tulain R, Hussain T, Amjad MW, Raja MAG, Farooq U, Aman W. Fabrication of thiolated chitosan based biodegradable nanoparticles of ticagrelor and their pharmacokinetics. Polym Polym Compos. 2022; 30:1-13.
28. Kisku A, Nishad A, Agrawal S, Paliwal R, Datusalia AK, Gupta G, Singh SK, Dua K, Sulakhiya K. Recent developments in intranasal drug delivery of nanomedicines for the treatment of neuropsychiatric disorders. Front Med. 2024; 11:1463976